J5.5

IMPROVING PRECIPITATION RETRIEVAL WITH NEXT GENERATION GPM RADAR AND RADIOMETER INSTRUMENTS

K.-S. Kuo*
Caelum Research Corporation, Rockville, Maryland
Eric A. Smith
NASA Goddard Space Flight Center, Greenbelt, Maryland
Ziad S. Haddad, Eastwood Im
NASA Jet Propulsion Laboratory, Pasadena, California
Alberto Mugnai
Institute of Atmospheric Physics, National Research Council, Rome, Italy

1. INTRODUCTION

Onboard the core satellite, the centerpiece of the newly authorized Global Precipitation Measurement (GPM) mission, will be a dual-frequency radar transmitting at 13.6 and 35 GHz frequencies in addition to a TRMM-like radiometer with expanded capabilities. The dual-frequency capability of the radar is expected to take precipitation measurement beyond the accomplishments of the Tropical Rainfall Measurement Mission (TRMM). Although multi-frequency methods in general improve our rainfall retrievals over the single-frequency methods, their success is still limited. This paper intends to investigate the cause(s) of such underachievement and to embark on, hopefully, finding a remedy.

2. BACKGROUNDS

In the following discussion we limit our scope to liquid precipitation only. We assume that the only material reflecting or attenuating a radar pulse is the water droplets in the forms of rain and/or cloud. Moreover, we assume these droplets to be spherical. These assumptions should and will be relaxed in future investigations.

The radar retrieval of rainfall is based upon the return signal from the reflection of the radar pulse by the hydrometeors in the illuminated volume, which is normally expressed as *equivalent radar reflectivity factor* in mm^6m^{-3},

$$Z_e = \frac{10^6\lambda^4}{\pi^5\left|K_w\right|^2}\int_{r_{\min}}^{r_{\max}}\sigma_b(r)n(r)dr, \quad (1)$$

where λ is the wavelength (cm) used by the radar, K_w is the dielectric factor of water, $\sigma_b(r)$ is the backscatter cross section (cm^2) of a raindrop with radius r (cm), and $n(r)$ ($m^{-3}cm^{-1}$) is the droplet size distribution (*DSD*) in the volume illuminated by the radar pulse. Since the reflected signal is attenuated by the medium between the illuminated volume and the radar antenna, a closely related quantity is the *specific attenuation* (dB km^{-1}),

$$k = 0.434\int_{r_{\min}}^{r_{\max}}\sigma_e(r)n(r)dr, \quad (2)$$

**Corresponding author address:* K.-S. Kuo, NASA GSFC, Mail Stop 912.1, Greenbelt, MD 20771; email: kskuo@radar.gsfc.nasa.gov

whereas the mathematical expression for rainfall rate in mm/hr is

$$R \equiv 4.8\pi\int_{r_{\min}}^{r_{\max}} v(r)r^3n(r)dr, \quad (3)$$

where $v(r)$ is the fall speed of the raindrop with radius r. All three quantities are integrals involving the DSD. Therefore many of the radar precipitation retrieval methods seek to relate Z_e and k to R in simple analytical expressions. This results in many $Z-R$ relations reported in Battan (1973). However, there is no information in either Z_e or k about $v(r)$, which is usually a complicated function of air motion, hence most methods assume it to be the same as the fall speed in stagnant air, $v_0(r)$. The authors believe this is one of the causes in the limited success achieved by $Z-R$ relations.

Next, we turn our attention to a similar integral quantity also involving the DSD, the *liquid water content* (g/m^3),

$$W = \frac{4}{3}\pi\rho_w\int_{r_{\min}}^{r_{\max}} r^3n(r)dr, \quad (4)$$

which we have better hope of accurate retrieval without knowing anything concerning $v(r)$. Since the DSD, $n(r)$, is the underlining thread connecting (1), (2) and (4), many researchers (e.g. Marshall and Palmer, 1948; Ulbrich, 1983) therefore assume a certain distribution model for the DSD (e.g. exponential or gamma) and carry out precipitation retrieval based on it. However, the operands in the integrals of (1), (2) and (4) have different dependencies. Consequently different DSD's giving the same Z_e or k may yield different W values and, vice versa. It is this non-uniqueness that has plagued the progress in radar rainfall retrieval in general. This non-uniqueness, the authors believe, is another major cause to the myriad of different $Z-R$ relationships.

In as early as the 1950s, Atlas and colleagues (Atlas, 1954; Atlas and Chmela, 1957 and references thereof) find that, when Rayleigh approximation is valid, the radar reflectivity factor Z (mm^6m^{-3}) can be expressed in terms of liquid water content, W (g/cm^3), median volume diameter, D_0 (cm), and G as

$$Z = \frac{6\times10^6}{\pi\rho_w} D_0^3 W G \tag{5}$$

where

$$G = \frac{\int_0^{D_{\max}} D^6 N(D) dD}{D_0^3 \int_0^{D_{\max}} D^3 N(D) dD}$$

is a dimensionless measure of the breadth of the DSD. One can easily verity that the above relation holds regardless of the distribution model assumed, i.e. it is true for any DSD. In other words, the three parameters: W, D_0 and G uniquely characterize the DSD in determining Z. In this investigation we venture to find such characteristic parameters suitable for the GPM radar frequencies where Rayleigh approximation may no longer be valid.

3. METHODOLOGY

In the optical wavelengths, Hansen and Travis (1974) propose using *effective radius* and *effective variance*, defined as

$$r_e = \frac{\int_{r_{\min}}^{r_{\max}} r^3 n(r) dr}{\int_{r_{\min}}^{r_{\max}} r^2 n(r) dr} \tag{6}$$

and

$$v_e = \frac{\int_{r_{\min}}^{r_{\max}} r^4 n(r) dr}{r_e^2 \int_{r_{\min}}^{r_{\max}} r^2 n(r) dr} - 1 \tag{7}$$

respectively, for cloud microphysical retrievals. Since the size parameter, $2\pi r/\lambda$, is comparable (especially at the 35 GHz frequency) these are the first candidates in our search for characteristic DSD parameters. The results, not surprisingly, turn out to be very encouraging.

We start with a very general formulation for droplet size distributions, a combination of two modified gamma distribution, which is capable of producing the bimodal feature often observed in rain,

$$\begin{aligned} n(r) = \eta^{-1}_{\mu,\kappa,z_{1,\min},z_{1,\max}} \kappa \left(\frac{r}{r_{c,1}}\right)^{\mu} \exp\left[-\left(\frac{r}{r_{c,1}}\right)^{\kappa}\right]\left(\frac{fN_T}{r_{c,1}}\right) \\ + \eta^{-1}_{\mu,\kappa,z_{2,\min},z_{2,\max}} \kappa \left(\frac{r}{r_{c,2}}\right)^{\mu} \exp\left[-\left(\frac{r}{r_{c,2}}\right)^{\kappa}\right]\left(\frac{(1-f)N_T}{r_{c,2}}\right), \end{aligned} \tag{8}$$

where μ and κ are dimensionless parameters of the distribution, N_T is the total number concentration, f is a fraction between 0 and 1, $r_{c,1}$ and $r_{c,2}$ ($r_{c,1} < r_{c,2}$) are the *characteristic radii* for the first and second modified gamma distributions respectively,

$$\begin{aligned} \eta_{\mu,\kappa,z_{\min},z_{\max}} &= \eta\left(\mu,\kappa,z_{\min},z_{\max}\right) \\ &= \eta\left[\mu,\kappa,\left(\frac{r_{\min}}{r_c}\right),\left(\frac{r_{\max}}{r_c}\right)\right] \\ &= \gamma\left(\frac{\mu+1}{\kappa}, z_{\max}\right) - \gamma\left(\frac{\mu+1}{\kappa}, z_{\min}\right), \end{aligned}$$

and γ is the *incomplete gamma function*,

$$\gamma(x,\alpha) \equiv \int_0^{\alpha} t^{x-1} e^{-t} dt.$$

In our investigation we set $r_{\min} = 0$. Even with this constraint, such a DSD model allows no fewer than six adjustable parameters (excluding N_T, for reasons that become clear later): μ, κ, f, $r_{\max}$, $r_{c,1}$, and $r_{c,2}$, so that one may have confidence that it will approximate any natural DSD well.

With (8) as our model for DSD we may evaluate W, r_e and v_e to be

$$W = \frac{4}{3}\pi\rho_w H(3) N_T r_{c,1}^3, \tag{9}$$

$$r_e = \frac{\mathrm{H}(3)}{\mathrm{H}(2)} r_{c,1} \quad \text{and} \quad v_e = \frac{\mathrm{H}(2)\mathrm{H}(4)}{\left[\mathrm{H}(3)\right]^2} - 1, \tag{10}$$

where

$$\begin{aligned} \mathrm{H}(m) &\equiv H\left(m,\mu,\kappa,f,r_{c,1},r_{c,2},r_{\min},r_{\max}\right) \\ &= f\,\frac{\eta_{\mu+m,\kappa,z_{1,\min},z_{1,\max}}}{\eta_{\mu,\kappa,z_{1,\min},z_{1,\max}}} + (1-f)\,\frac{\eta_{\mu+m,\kappa,z_{2,\min},z_{2,\max}}}{\eta_{\mu,\kappa,z_{2,\min},z_{2,\max}}}\left(\frac{r_{c,2}}{r_{c,1}}\right)^m. \end{aligned}$$

We notice that N_T is not present in the formulation of either r_e or v_e. In other words, when a distribution is chosen by fixing the other parameters, N_T only serves to modify the value of W. The value of r_e or v_e is not

Category	Type	f	$r_{c,2}/r_{c,1}$	$r_{\max}$ (mm)
1.	Mono-modal	1	1	20
2.	Mono-modal	1	1	15
3.	Bimodal	0.5	5	15
4.	Bimodal	0.3	5	15
5.	Bimodal	0.3	10	15

Table 1. Distribution parameters for the five categories of distributions.

affected by N_T at all.

In our simulations we systematically vary v_e from 0.1 to 0.5 with a 0.1 increment. For each value of v_e we vary r_e among the values of 0.25, 0.5, 1, 2 and 4 mm. For each paired values of (r_e, v_e), a parameter-finding procedure finds, in each of the five categories listed in Table 1, the distribution parameters: μ, κ, $r_{c,1}$ and $r_{c,2}$ for a number of distributions yielding the desired r_e and v_e values. Three distributions are then randomly selected in each distribution category from those found by the parameter-finder. This results in fifteen (15) distributions for each pair of (r_e, v_e). For the reason mentioned above, the total number concentration, N_T, is adjusted so that the liquid water content is held constant at 1 g/m^3 in our later discussions unless explicitly stated otherwise.

4. RESULTS

Figure 1 displays fifteen DSDs each in logarithmic scale for (r_e, v_e) of (1 mm, 0.2) in the upper panel and (2 mm, 0.2) in the lower panel. The difference among the distributions is quite obvious from the figure.

The upper panel of Figure 2 shows the reflectivity factors at 13.6 GHz (thick line) and 35 GHz (thin line) for the fifteen distributions with (r_e, v_e) of (0.25 mm, 0.5). It is rather difficult to detect variations in these lines, therefore their deviations from the means are plotted in the lower panel with thick lines connecting solid circles for 13.6 GHz and thin lines connecting open squares for 35 GHz. We pick this figure out of the 25 available because it exhibits the greatest variation in Z_e among all (r_e, v_e) combinations. Yet, the entire range of variation is only about 1 dB for 13.6 GHz and less than 0.5 dB for 36 GHz.

The variations of Z_e among distributions is depicted in a more comprehensive manner in the contour plot of Figure 3. The solid lines contour the average Z_e of the fifteen distributions as a function of (r_e, v_e) while the dotted lines contour the minimum Z_e of the distributions and the dashed lines the maximum. The closeness of the dotted and dashed contours to their corresponding solid ones demonstrates that, when liquid water content is held constant, (r_e, v_e) is a good predictor of Z_e. (The large separation for the 13.6 GHz near $r_e = 4$ mm, i.e. the boundary of our r_e domain, is mainly due to sparseness in data points (25 total), the slow change in Z_e values in this region, and an artifact of the contouring procedure used.)

The variations in specific attenuation, k, is even less. The greatest range of variation among the fifteen

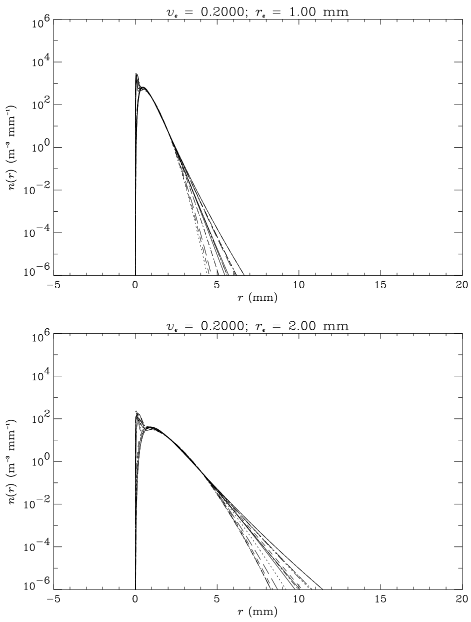

Figure 1. Droplet size distributions (DSDs) with effective radii of 1 mm (upper panel) and 2 mm (lower panel) and effective variance of 0.2.

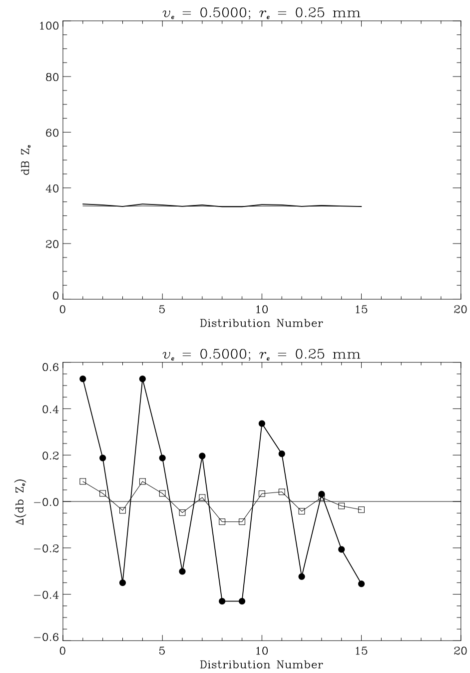

Figure 2. Variations in Z_e among the fifteen DSDs for v_e = 0.5 and r_e = 0.25 mm.

distributions occurs at (r_e, v_e) of (2 mm, 0.2) and it is less than 0.2 dB. In a similar figure as Fig. 3 (not shown), the tightness among the contours of different line styles is more pronounced that that shown in Fig. 3. This means that the variations caused by differences in distributions are less in k than in Z_e across the entire range of (r_e, v_e) values.

Now, we take a look at the influence of W. Figure 4 shows the combined influence of r_e and W simultaneously on Z_e for both frequencies at a constant v_e of 0.1. Five diagonal lines are isopleths of r_e equal to 0.25, 0.5, 1, 2 and 4 mm from left to right respectively. (The isopleths 0.25 and 0.5 mm are too close together for distinction.) Each of these lines connects the Z_e values for of 0.1, 0.266, 0.707, 1.88 and 5 g/m^3 from lower-left to upper-right respectively. The constant W values are also connected by line segments to make the grid-like appearance in the figure. The closeness of the isopleths for $r_e \le 0.5$ mm may explain the difficulties of radar remote sensing encountered in light rain situations. Because a DSD with a smaller W and a larger r_e may be interpreted as one with a larger W and a smaller r_e, it leads to error in the R estimate. Although the isopleths of smaller r_e values grow apart as v_e increases (not shown), remembering that v_e is a measure of the breadth of the DSD one expects a smaller v_e for light rains.

The non-uniqueness in k for smaller r_e and v_e values is worse than that in Z_e. However, it appears that, within the errors shown in Fig. 2, there is almost a one-to-one correspondence between $(Z_{e,13.6}, Z_{e,35})$ [or $(k_{13.6}, k_{35})$] and (r_e, W) for $r_e > 1$ mm when v_e is known.

5. CONCLUSIONS

We find in this study that, as far as equivalent radar reflectivity factor and specific attenuation are concerned, the three parameters r_e, v_e, and W characterize the droplet size distribution more adequately than parameters currently used in radar precipitation retrievals. In other words, it doesn't matter what DSD models one assumes; as long as the distributions have the same r_e, v_e, and W they yield roughly the same Z_e and k in the two frequencies of 13.6 and 35 GHz. Such a framework also sheds light on the causes for the usual difficulties encountered in radar rainfall retrieval, such as the copious $Z-R$ relations and the particular inaccuracies in light rain situations. Furthermore, it facilitates better characterization of retrieval errors.

6. REFERENCES

Atlas, D., 1954: The estimation of cloud parameters by radar. *J. Meteorol.*, **11**, 309-317.

Atlas, D., and A. C. Chmela, 1957: Physical-synoptic variations of drop-size parameters. *Proceedings, Sixth Weather Radar Conference*, 21-30.

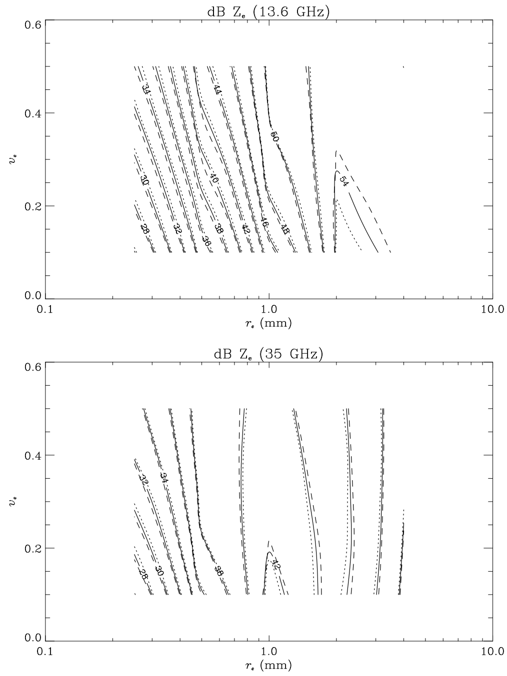

Figure 3. Contours of mean, minimum, and maximum Z_e of the fifteen DSDs as a function of r_e and v_e.

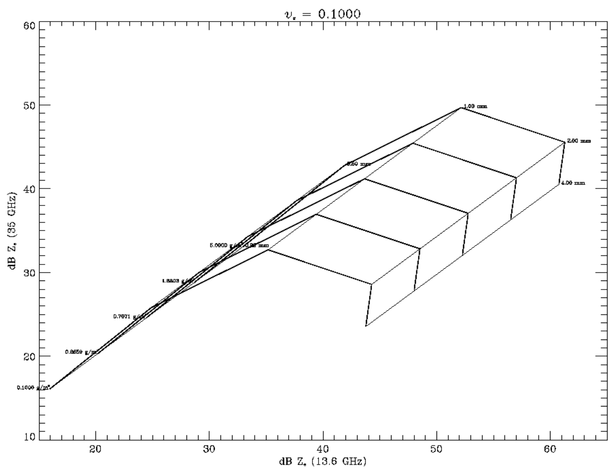

Figure 4. Bi-spectral Z_e as a function of $v(f)$ and W.

Battan, L. J., 1973: *Radar Observation of the Atmosphere*. University of Chicago Press, 342pp.

Hansen, J. E., and L. D. Travis, 1974: Light scattering in planetary atmosphere. *Space Science Review*, **16**, 527-610.

Marshall, J. S., and W. M. K. Palmer, 1948: The distribution of raindrops with size. *J. Meteorol.*, **5**, 165-166.

Ulbrich, C. W., 1983: Natural variations in the analytical form of the raindrop size distribution. *J. Climate Appl. Meteorol.*, **2**, 1764-1775.